A Preliminary Investigation of Decentralized Control for Satellite Formations*

J. Russell Carpenter
NASA Goddard Space Flight Center
Code 572
Greenbelt, MD 20771
(301) 286–7526
russell.carpenter@gsfc.nasa.gov

Abstract— A distributed satellite formation consisting of n nodes interconnected via a communications network could be controlled using a decentralized controller framework that operates in parallel over the network. For such problems, a solution that minimizes data transmission requirements, in the context of linear-quadratic control theory, was given by Speyer [1]. An investigation of the feasibility of such an approach to satellite formation flying is currently being undertaken, in the context of efforts sponsored by NASA and the Air Force to develop architectures, strategies, and control approaches for various proposed distributed satellite missions. Among the issues under investigation are the effects of command and data handling system and communications channel noise and latency. For example, it is likely that the measurement devices and/or their associated command and data handling systems may provide asynchronous and/or non-simultaneous measurement data. It is also probable that transmission of the data between nodes could be delayed one or more sampling periods and/or interrupted for extended intervals. Furthermore, since it is not possible to create a noise-free communications channel, errors in the transmitted data will be introduced at the level of the network, in addition to errors introduced at the measurement and state transition levels. An additional difficulty is that, in general, nonlinearities in the dynamics and measurements of the distributed satellite control problem require the use of ad-hoc procedures such as the extended Kalman filter. Therefore, a simulation methodology is adopted for the study of the aforementioned issues in this work.

Table of Contents

1. Introduction

A decentralized framework for linear-quadratic-Gaussian (LQG) control is investigated for applicability to autonomous satellite formations. For such problems, a solution that minimizes data transmission requirements has been given by Speyer [1]. In reference [1], the decentralized estimator was placed in an LQG control setting. Since then other decentralized control algorithms have been analyzed which consider one-step delayed-information sharing patterns. In reference [2], the decentralized LQG control is extended to the decentralized linear-exponential-Gaussian control which is related to deterministic $\mathcal{H}_\infty$ control synthesis. Other generalizations of reference [1] may be found in references [3] and [4], and in reference [5], this work served as the basis for a fault-tolerant multi-sensor navigation architecture.

The decentralized LGQ framework is non-hierarchical, and coordination by a central supervisor is not required. Detected failures degrade the system performance gracefully. Each node in the decentralized network processes only its own measurement data, in parallel with the other nodes. Although the total computational burden over the entire network is greater than it would be for a single, centralized controller, fewer computations are required locally at each node. Requirements for data transmission between nodes are limited to only the dimension of the control vector, at the cost of maintaining a local additional data vector. The data vector compresses all past measurement history from all the nodes into a single vector of the dimension of the state. The approach is optimal with respect to standard LQG cost function.

As literally formulated in reference [1], the approach is valid for linear time-invariant (LTI) systems only. As with the standard LQG problem, extension to linear time-varying (LTV) systems requires that each node propagate its filter covariance forward and controller Riccati matrix backward at each time step. Extension to non-linear systems can also be accomplished via linearization about a reference trajectory in the standard fashion, or linearization about the current state estimate as with the extended Kalman filter. Each of these extensions induces additional local processing and data transmission requirements, however.

To investigate the feasibility of the decentralized approach to satellite formation flying, an existing centralized LQG design for a single spacecraft orbit control problem is adapted to the decentralized framework. The existing design uses a fixed reference trajectory, and by appropriate choice of coordinates and simplified measurement modeling is formulated as a linear time-invariant system.

The remainder of this paper is organized as follows. The next two sections briefly describe the decentralized control approach of reference [1] and the simplified spacecraft orbit control LQG design, respectively. The next section presents and discusses results for a particular three satellite formation, and highlights a few issues relevant to this problem. The final section discusses the feasibility of extending this work to the kind of time-varying models required for use in an actual distributed spacecraft application.

2. BACKGROUND

Reference [1] considers the solution to the discrete (a continuous-time solution is also given) decentralized LQG control problem, described by the minimization of

$$J = \min_{\mathbf{u}_i^j} \mathrm{E}\left[\frac{1}{2}\sum_{i=1}^{N}\left\{\mathbf{x}_i^{\mathsf{T}}\mathbf{Q}_i\mathbf{x}_i + \sum_{j=1}^{K}(\mathbf{u}_i^j)^{\mathsf{T}}\mathbf{R}_i^j\mathbf{u}_i^j\right\}\right], \quad j = 1,2,\ldots,K; i = 1,2,\ldots,N, \tag{1}$$

subject to the linear time invariant measurement update given by

$$\mathbf{y}_i^j = \mathbf{H}^j\mathbf{x}_i + \mathbf{v}_i^j, \tag{2}$$

and the linear time invariant state update given by

$$\mathbf{x}_{i+1} = \mathbf{\Phi}\mathbf{x}_i + \sum_{j=1}^{K}\mathbf{B}^j\mathbf{u}_i^j + \mathbf{w}_i, \tag{3}$$

where $\mathbf{x}_1 \sim N(\bar{\mathbf{x}}, \bar{\mathbf{P}})$, $\mathbf{w}_i \sim N(\mathbf{0}, \mathbf{W}_i\delta_{i\ell})$, $\mathbf{v}_i^j \sim N(\mathbf{0}, \mathbf{V}_i^j\delta_{i\ell})$, and where K is the number of nodes in the network, and N is the number of epochs over which the system operates. Also, $\mathbf{u}$ is the control vector, $\mathbf{y}$ is the measurement vector, $\mathbf{x}$ is the state vector, $\mathbf{w}$ is the process noise vector, and $\mathbf{v}$ is the measurement noise vector. Figure 1 illustrates the approach taken by reference [1].

The solution is based on the decomposition of the state into $\mathbf{x}_i^C$, that depends only on the control, and $\hat{\mathbf{x}}_i^D$, that depends only on the incoming data. The global Riccati matrices $\mathbf{P}$ and $\mathbf{S}$ are computed off-line via

$$\mathbf{P}_{i+1}^{-1} = \mathbf{M}_{i+1}^{-1} + \sum_{j=1}^{K}(\mathbf{H}^j)^{\mathsf{T}}(\mathbf{V}_{i+1}^j)^{-1}\mathbf{H}^j \tag{4}$$

$$\mathbf{M}_{i+1} = \mathbf{\Phi}\mathbf{P}_i\mathbf{\Phi}^{\mathsf{T}} + \mathbf{W}_i; \qquad \mathbf{M}_1 = \bar{\mathbf{P}} \tag{5}$$

$$\mathbf{S}_i = \mathbf{\Phi}^{\mathsf{T}}\mathbf{S}_{i+1}\mathbf{\Phi} - \sum_{j=1}^{K}(\mathbf{L}_i^j)^{\mathsf{T}}(\mathbf{R}^j + (\mathbf{B}^j)^{\mathsf{T}}\mathbf{S}_{i+1}\mathbf{B}^j)\mathbf{L}_i^j + \mathbf{Q}_i, \quad \mathbf{S}_N = \mathbf{0}, \tag{6}$$

where

$$\mathbf{L}_i^j = -(\mathbf{R}^j + (\mathbf{B}^j)^{\mathsf{T}}\mathbf{S}_{i+1}\mathbf{B}^j)^{-1}(\mathbf{B}^j)^{\mathsf{T}}\mathbf{S}_{i+1}. \tag{7}$$

The local filter covariance matrix, $\mathbf{P}_i^j$, is also computed offline via

$$\mathbf{P}_{i+1}^{-1} = \mathbf{M}_{i+1}^{-1} + (\mathbf{H}^j)^{\mathsf{T}}(\mathbf{V}_{i+1}^j)^{-1}\mathbf{H}^j \tag{8}$$

$$\mathbf{M}_{i+1}^j = \mathbf{\Phi}\mathbf{P}_i^j\mathbf{\Phi}^{\mathsf{T}} + \mathbf{W}_i; \qquad \mathbf{M}_1 = \bar{\mathbf{P}}. \tag{9}$$

The vectors $\mathbf{h}_i^j$ are data-dependent vectors that efficiently compress non-local information. The vectors $\boldsymbol{\alpha}_i^{\ell j}$ are transmission vectors that have the dimensions of the control vectors.

Note that the only information that need be exchanged over the network are vectors that have the dimensions of the controls. The local control $\mathbf{u}_i^j$ cannot be computed until $\boldsymbol{\alpha}_i^{j\ell}, \ell = 1,2,\ldots,j-1,j+1,\ldots,K$ that are received from the network at junction $\mathcal{B}$ have been computed at all the other nodes' junctions $\mathcal{C}$ (see Figure 1). If $\mathbf{B}^j$ are all the same, then $\mathbf{u}_i^j$ are all the same, so the sum at junction $\mathcal{A}$ does not require a network connection, and the $\mathbf{u}_i^j$ need not be exported to the network.

If the solution approach is used for decentralized control of a distributed satellite cluster, there are a few potential issues. Each node may be associated with only a partition of the global state. However, this is shown not to be a limitation in reference [3]. The system may be time-varying, so that the Riccati matrices become data-dependent, and may not be computed off-line. A terminal penalty function may be present in the cost function, J. Finally, it may not be possible to accommodate transmission of the $\boldsymbol{\alpha}_i^{\ell j}$ and reception of the $\boldsymbol{\alpha}_i^{j\ell}$ all during the current stage i.

3. LQG DESIGN

The following subsections describe the design objectives, system linearization and discretization, tracking law, estimator design, and modifications required to the standard LQ design to accommodate the decentralized approach.

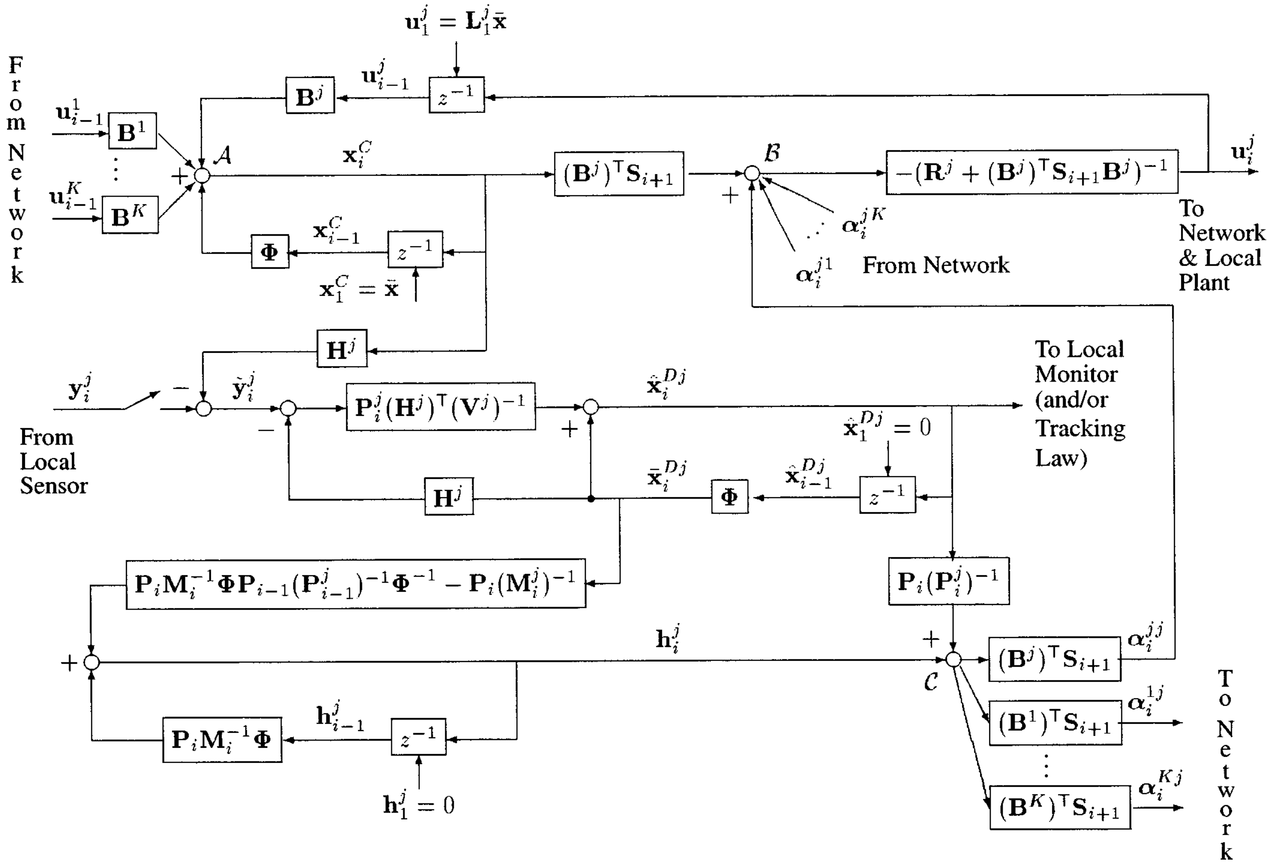

Figure 1: Block Diagram of Speyer's Solution for Decentralized LQG Control of a Linear Time-Invariant Plant

Objectives

The time-varying linear-quadratic regulator (LQR) minimizes the criterion

$$J = \int_{t_1}^{t_N} \left[\mathbf{x}(\tau)^{\mathsf{T}}\mathbf{Q}(\tau)\mathbf{x}(\tau) + \mathbf{u}(\tau)^{\mathsf{T}}\mathbf{R}(\tau)\mathbf{u}(\tau)\right] d\tau + \mathbf{x}(t_N)^{\mathsf{T}}\mathbf{S}_N\mathbf{x}(t_N) \tag{10}$$

with respect to the linear, time-varying (LTV) system

$$\dot{\mathbf{x}}(t) = \mathbf{A}(t)\mathbf{x}(t) + \mathbf{B}(t)\mathbf{u}(t); \quad \mathbf{x}(t_1) = \mathbf{x}_1. \tag{11}$$

The time-varying matrices $\mathbf{Q}(\tau), \mathbf{R}(\tau) : \mathbf{Q}(\tau) \geq 0, \mathbf{R}(\tau) > 0, \tau \in [t_1, t_N]$, act as penalty functions on the states, $\mathbf{x}(t)$, and the controls, $\mathbf{u}(t)$, respectively. Additionally, the matrix $\mathbf{S}_N : \mathbf{S}_N \geq 0$ forms a penalty on the final states. Because the weighting matrices in the LQR framework are arbitrary, this framework represents a class of optimal regulators. In order to choose the controller, the following additional performance metrics are defined:

$$\pi_p = \sup_{j\in\mathcal{J}_p} \|\mathbf{x}_j(t)\|_\infty; \quad \mathcal{J}_p \sim \text{position channels} \tag{12}$$

$$\pi_v = \sup_{j\in\mathcal{J}_v} \|\mathbf{x}_j(t)\|_\infty; \quad \mathcal{J}_v \sim \text{velocity channels} \tag{13}$$

$$\pi_u = \sup_{j\in\mathcal{J}_u} \frac{1}{N}\sqrt{\sum_i^N \mathbf{u}_j^2(t_i)}; \quad \mathcal{J}_u \sim \text{control channels}, \; N \sim \text{signal length} \tag{14}$$

The basis for the first two criteria, π_p and π_v, is to identify the controller design which generates the smallest maximum value of the states corresponding to position and velocity. The third criterion, π_u, represents the maximum among the mean square values of the controls, and is based on the total "control effort."

Linearization of System Dynamics

Before a controller can be designed, the dynamics of the distributed satellites' orbits must be expressed in the form of an

LTV system, as specified by Eq. (11). Since these dynamics are represented by a high-order, nonlinear, nonconservative system of differential equations, appropriate simplifying assumptions must be used to achieve reductions in mathematical complexity. Then, linearization of the resulting simple nonlinear equations about a reference orbit is employed to achieve a linear, time-invariant system, which forms a subclass of the systems represented by Eq. (11).

The satellites are assumed to be orbiting the earth in a near-equatorial, near-circular orbit. Each satellite is further assumed to remain in the vicinity of a point, the *formation origin*, that orbits the earth in an equatorial, circular orbit. Its position is specified by the spherical coordinates r^0, θ^0, and ϕ^0, defined in Figure 2(a). It is also assumed that each satellite has small thrusters that it can use to apply accelerations u_r, u_θ, and u_ϕ in the $\hat{r}$, $\hat{\theta}$, and $\hat{\phi}$ (radial, downtrack, and crosstrack) directions, defined in Figure 2(b). A state vector and control vector are chosen for each satellite $j = 1, 2, \ldots, K$ (for $j = 0$, the state vector refers to the formation origin) as follows:

$$\mathbf{X}^j = \left[r^j,\ \dot{r}^j,\ \theta^j,\ \dot{\theta}^j,\ \phi^j,\ \dot{\phi}^j\right]^{\mathsf{T}}, \qquad j = 0, 1, 2, \ldots, K \tag{15}$$

$$\mathbf{U} = \left[u_r^j,\ u_\theta^j,\ u_\phi^j\right]^{\mathsf{T}}, \qquad j = 1, 2, \ldots, K \tag{16}$$

Each satellite's position relative to the formation origin is therefore given by

$$\mathbf{x}^j = \mathbf{X}^j - \mathbf{X}^0, \tag{17}$$

as Figure 2(b) depicts.

In terms of the states chosen above, the satellite dynamics may be expressed as a first-order, non-linear, autonomous, vector differential equation of the form

$$\dot{\mathbf{X}}^j = \mathbf{f}(\mathbf{X}^j, \mathbf{U}^j), \tag{18}$$

where

$$\mathbf{f}(\mathbf{X}^j, \mathbf{U}^j) = \left[\begin{array}{c} \dot{r} \\ -\frac{\mu}{r^2} + r\dot{\phi}^2 + r\dot{\theta}^2 \cos^2\phi + \frac{u_r}{m} \\ \dot{\theta} \\ -2\dot{r}\dot{\theta}/r + 2\dot{\phi}\dot{\theta}\tan\phi + \frac{u_\theta}{mr} \\ \dot{\phi} \\ -2\dot{r}\dot{\phi}/r - \dot{\theta}^2\cos\phi\sin\phi + \frac{u_\phi}{mr} \end{array}\right]_j . \tag{19}$$

In order to linearize the system of Eq. (19), the partial derivatives of f with respect to the states and controls are required. To simplify the notation, the parameter n, known as the *mean motion*, or *orb-rate*, which is defined by

$$n = \sqrt{\frac{\mu}{r^3}}, \tag{20}$$

will be employed. Now, defining the *state sensitivity matrix* as

$$\mathbf{A}^j = \frac{\partial \mathbf{f}(\mathbf{X}^j, \mathbf{U}^j)}{\partial \mathbf{X}^j}, \tag{21}$$

then

$$\mathbf{A}^j = \left[\begin{array}{cccccc} 0 & 1 & 0 & 0 & 0 & 0 \\ (\dot{\phi}^2 + 2n^2 + \dot{\theta}^2\cos^2\phi) & 0 & 0 & 2r\dot{\theta}\cos^2\phi & -2r\dot{\theta}^2\cos\phi\sin\phi & 2r\dot{\phi} \\ 0 & 0 & 0 & 1 & 0 & 0 \\ 2\dot{r}\dot{\theta}/r^2 & -2\dot{\theta}/r & 0 & 2(\dot{\phi}\tan\phi - \dot{r}/r) & 2\dot{\phi}\dot{\theta}\sec^2\phi & 2\dot{\theta}\tan\phi \\ 0 & 0 & 0 & 0 & 0 & 1 \\ 2\dot{r}\dot{\phi}/r^2 & -2\dot{\phi}/r & 0 & -2\dot{\theta}\cos\phi\sin\phi & \dot{\theta}^2\cos 2\phi & -2\dot{r}/r \end{array}\right]_j \tag{22}$$

Defining the reference state trajectory,

$$\mathbf{X}_* = [r_*,\ 0,\ n_* t,\ n_*,\ 0,\ 0]^{\mathsf{T}}, \tag{23}$$

and the reference control $\mathbf{U}_* = [0, 0, 0]^{\mathsf{T}}$, where r_* is the reference radius, and n_* is the reference orb-rate, defined in terms of r_* per Eq. (20), a great deal of simplification results:

$$\mathbf{A}_* = \left.\frac{\partial \mathbf{f}(\mathbf{X}, \mathbf{U})}{\partial \mathbf{X}}\right|_{\mathbf{X}_*, \mathbf{U}_*} \tag{24}$$

$$= \left[\begin{array}{cccccc} 0 & 1 & 0 & 0 & 0 & 0 \\ 3n_*^2 & 0 & 0 & 2n_* r_* & 0 & 0 \\ 0 & 0 & 0 & 1 & 0 & 0 \\ 0 & -2n_*/r_* & 0 & 0 & 0 & 0 \\ 0 & 0 & 0 & 0 & 0 & 1 \\ 0 & 0 & 0 & 0 & -n_*^2 & 0 \end{array}\right]. \tag{25}$$

If the state vector is now redefined as

$$\tilde{\mathbf{X}}^j = \left[r^j,\ \dot{r}^j,\ r_*\theta^j,\ r_*\dot{\theta}^j,\ r_*\phi^j,\ r_*\dot{\phi}^j\right]^{\mathsf{T}} \tag{26}$$

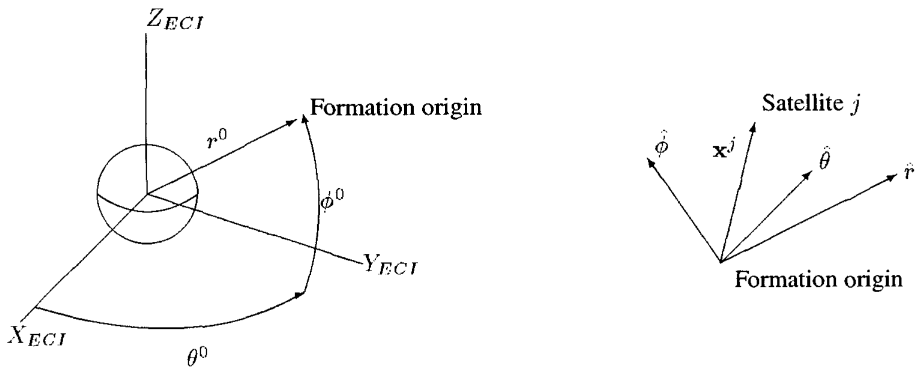

(a) (b)

Figure 2: Problem Geometry: (a) Position of formation origin relative to Earth-Centered Inertial (ECI) frame; (b) Position of jth satellite relative to formation origin

then the corresponding matrix $\tilde{A}_*$ is

$$\tilde{\mathbf{A}}_* = \begin{bmatrix} 0 & 1 & 0 & 0 & 0 & 0 \\ 3n_*^2 & 0 & 0 & 2n_* & 0 & 0 \\ 0 & 0 & 0 & 1 & 0 & 0 \\ 0 & -2n_* & 0 & 0 & 0 & 0 \\ 0 & 0 & 0 & 0 & 0 & 1 \\ 0 & 0 & 0 & 0 & -n_*^2 & 0 \end{bmatrix}. \tag{27}$$

Scaling the state vector in this fashion is motivated by computational issues. For almost any convenient set of units, r_* is apt to be quite large compared with n_*, which will cause wide disparities among the sizes of the elements of A_*. In addition to rectifying this problem, the chosen scaling has the cosmetic feature of expressing all the states in units of distance and time.

Finally, the *control sensitivity matrix* is

$$\mathbf{B}^j = \frac{\partial \mathbf{f}(\mathbf{X}^j, \mathbf{U}^j)}{\partial \mathbf{U}^j}, \tag{28}$$

so that, after evaluating the partial derivatives on the reference trajectory, and applying the same scaling given above,

$$\tilde{\mathbf{B}}_* = \begin{bmatrix} 1 & 0 & 0 \\ 0 & 0 & 0 \\ 0 & 1 & 0 \\ 0 & 0 & 0 \\ 0 & 0 & 1 \end{bmatrix} \tag{29}$$

Note that these assumptions have led to $\tilde{\mathbf{A}}_*$ and $\tilde{\mathbf{B}}_*$ that are the same for all nodes. Henceforth, the $\tilde{}$ and subscript $*$ notation will be dropped, and $\mathbf{A}$ and $\mathbf{B}$ will be understood to refer to $\tilde{\mathbf{A}}_*$ and $\tilde{\mathbf{B}}_*$, respectively.

Now deviations from the reference trajectory, defined by $\mathbf{x}^j = \mathbf{X}^j - \mathbf{X}_*$ and $\mathbf{u} = \mathbf{U}^j - \mathbf{U}_*$, may be written as a linear system as follows:

$$\dot{\mathbf{x}}^j = \mathbf{A}\mathbf{x}^j + \mathbf{B}\mathbf{u}^j. \tag{30}$$

This has the form of the linear dynamic system required for the LQR design (cf. Eq. (11).) Note that the $\mathbf{x}^j$ defined above is consistent with the definition in Figure 2(b), since the formation origin is assumed to follow the reference trajectory.

Discretization

To discretize this system, first consider the solution of the unforced system, $\dot{\mathbf{x}}^j(t) = \mathbf{A}\mathbf{x}^j(t)$:

$$\mathbf{x}^j(t) = \mathbf{\Phi}(t, t_1)\mathbf{x}^j(t_1), \tag{31}$$

where $\mathbf{\Phi}(t, t_1)$ is the state transition matrix. It can be shown (e.g. see Kaplan [6]) that $\mathbf{\Phi}(t, t_1) = \mathbf{\Phi}(n, \Delta t)$ for the two-body satellite problem, where

$$\mathbf{\Phi}(n, \Delta t) = \begin{bmatrix} \mathbf{\Phi}_{r,\theta}(n, \Delta t) & 0 \\ 0 & \mathbf{\Phi}_{\phi}(n, \Delta t) \end{bmatrix}, \tag{32}$$

$$\mathbf{\Phi}_{r,\theta}(n, \Delta t) = \begin{bmatrix} 4 - 3\cos n\Delta t & \frac{1}{n}\sin n\Delta t & 0 & \frac{2}{n}(1 - \cos n\Delta t) \\ 3n \sin n\Delta t & \cos n\Delta t & 0 & 2\sin n\Delta t \\ 6(\sin n\Delta t - 1) & \frac{2}{n}(\cos n\Delta t - 1) & 1 & \frac{4}{n}\sin n\Delta t - 3t \\ 6n(\cos n\Delta t - 1) & -2\sin n\Delta t & 0 & 4\cos n\Delta t - 3 \end{bmatrix}, \tag{33}$$

and

$$\Phi_{\phi}(n, \Delta t) = \begin{bmatrix} \cos n\Delta t & \frac{1}{n}\sin n\Delta t \\ -n \sin n\Delta t & \cos n\Delta t \end{bmatrix}. \quad (34)$$

Here n is the orb-rate, defined previously, and $\Delta t = t - t_1$. Thus, once n and Δt are specified, Φ is a constant matrix.

Using this unforced solution, the discrete form of Eq. (30) may be written as

$$\mathbf{x}_{i+1}^j = \Phi(n_*, t_{i+1} - t_i)\mathbf{x}_i^j + \Lambda\mathbf{u}_i^j \quad (35)$$

where

$$\Lambda\mathbf{u}_i^j = \int_{t_i}^{t_{i+1}} \Phi(n_*, \Delta\tau)\mathbf{B}\mathbf{u}^j(\tau)d\tau, \quad (36)$$

To evaluate the integral, model $\mathbf{u}^j(t)$ as

$$\mathbf{u}_i^j = \Delta\mathbf{v}_i^j \delta(t_i)dt, \quad (37)$$

where $\Delta\mathbf{v}_i^j$ is an impulsive velocity change assumed to occur at time t_i.

The system model that has been derived is linear time-invariant. Therefore, as in reference [1], the Riccati matrices $\mathbf{S}_i$ and control gains $\mathbf{L}_i^j$ may be computed off-line. This would not likely be true for realistic formation flying applications, especially those involving highly elliptic orbits.

Tracking Desired Local Trajectories

The LQR framework provides a regulator, that is, a controller that drives state deviations to zero. For the distributed satellite control problem, one actually wishes to have each of the nodes track a desired local trajectory relative to the formation origin, denoted $\mathbf{x}_d^j(t_i)$. Thus, the objective is to drive $\mathbf{x}^j(t_i) - \mathbf{x}_d^j(t_i)$ to zero. Reference [7] shows that if

$$\dot{\mathbf{x}}_d(t_i) = \mathbf{A}\mathbf{x}_d(t_i), \quad (38)$$

then the control law

$$\mathbf{u}_i = \mathbf{L}_i[\mathbf{x}(t_i) - \mathbf{x}_d(t_i)], \quad (39)$$

where $\mathbf{L}_i$ is the LQ gain matrix, will achieve the desired objective. If $\mathbf{x}_d(t_i)$ does not satisfy this condition, then the LQ cost function must be converted into an equivalent disturbance rejection problem [7], where the disturbance is $\mathbf{d}(t) = \mathbf{A}\mathbf{x}_d(t) - \dot{\mathbf{x}}_d(t)$.

In terms of the satellite control problem, this can be interpreted as requiring that the desired local trajectory be a free orbital trajectory. Several recent works (e.g., [8], [9], [10], [11]) have shown that for formation keeping to be economically feasible, the desired local trajectories should be free orbital trajectories, as nearly as possible. Use of the standard LQR framework imposes the necessity of this desirable condition.

Discrete Linear Kalman Filter Design

According to the certainty equivalence principle, the LQR design presented above is the optimal controller design, if the deviations from the reference trajectory result from Gaussian stochastic processes. However, to implement this design as an optimal control law, one must use an estimate of the state deviations that is based on observations of these random processes. Such an estimate is provided by the Kalman filter. Although in the satellite problem considered here, the state deviations do not result from stochastic processes, but rather from unmodeled dynamics, the implementation strategy suggested by the certainty equivalence principle will be employed.

Propagation Model— Assuming that the state deviations are indeed governed by the linear system used for the controller design, driven by white Gaussian noise, leads to the continuous model

$$\dot{\mathbf{x}}^j(t) = \mathbf{A}\mathbf{x}^j(t) + \mathbf{B}\mathbf{u}^j(t) + \mathbf{w}^j(t), \quad (40)$$

with $\mathbf{x}^j(t_1) = \bar{\mathbf{x}}^j$, $\mathbf{P}(t_1) = \mathrm{E}\big[(\bar{\mathbf{x}}^j - \mathrm{E}[\bar{\mathbf{x}}^j])(\bar{\mathbf{x}}^j - \mathrm{E}[\bar{\mathbf{x}}^j])^{\mathsf{T}}\big]$, $\mathbf{u}^j(t)$ specified, and $\mathrm{E}\big[\mathbf{w}^j(t)\big] = \mathbf{0}$, $\mathrm{E}\big[\mathbf{w}^j(t)(\mathbf{w}^j)^{\mathsf{T}}(\tau)\big] = \mathbf{W}^j\delta(t-\tau)$.

Using Eq. (35), the discrete form of Eq. (40) may be written as

$$\mathbf{x}_{i+1}^j = \Phi\mathbf{x}_i^j + \Lambda\mathbf{u}_i^j + \mathbf{w}_i^j, \quad (41)$$

where

$$\mathbf{w}_i^j = \int_{t_i}^{t_{i+1}} \Phi(\Delta\tau)\mathbf{w}^j(\tau)d\tau, \quad (42)$$

with

$$\begin{aligned} \mathrm{E}\Big[\mathbf{w}_i^j(\mathbf{w}_i^j)^{\mathsf{T}}\Big] &= \int_{t_i}^{t_{i+1}} \Phi(\Delta\tau)\mathbf{W}^j\Phi^{\mathsf{T}}(\Delta\tau)d\tau, \\ \mathrm{E}\Big[\mathbf{w}_i^j(\mathbf{w}_\ell^j)^{\mathsf{T}}\Big] &= \mathbf{0}. \end{aligned} \quad (43)$$

To evaluate this integral, a simplification is introduced. *For purposes of evaluating the process noise integral only*, the state is assumed to propagate according to $\mathbf{x}_{i+1}^j = \mathbf{x}_i^j + \dot{\mathbf{x}}_i^j\Delta t$. This results in an approximate state transition matrix,

$$\tilde{\Phi}(\Delta t) = \begin{bmatrix} 1 & \Delta t & 0 & 0 & 0 & 0 \\ 0 & 1 & 0 & 0 & 0 & 0 \\ 0 & 0 & 1 & \Delta t & 0 & 0 \\ 0 & 0 & 0 & 1 & 0 & 0 \\ 0 & 0 & 0 & 0 & 1 & \Delta t \\ 0 & 0 & 0 & 0 & 0 & 1 \end{bmatrix}. \quad (44)$$

Next, consider that since the state noise is used to account for unmodeled forces, it typically has non-zeros entries only for acceleration channels. If one further restricts the state noise to be uncorrelated between the various acceleration channels, $\mathbf{W}$ then has a diagonal structure, e.g.

$$\mathbf{W}^j = \text{diag}(0, w_{\ddot{r}}, 0, w_{r\ddot{\theta}}, 0, w_{r\ddot{\phi}}), \qquad (45)$$

which is here restricted to be the same for all nodes for simplicity, but this is not necessary. Then,

$$\mathbf{W}_i^j = \mathrm{E}\left[\mathbf{w}_i^j(\mathbf{w}_i^j)^\mathsf{T}\right] = \int_{t_i}^{t_{i+1}} \tilde{\mathbf{\Phi}}(\Delta\tau)\mathbf{W}^j\tilde{\mathbf{\Phi}}^\mathsf{T}(\Delta\tau)d\tau, \qquad (46)$$

so that

$$\mathbf{W}_i^j = \begin{bmatrix} w_{\ddot{r}}\Delta t^3/3 & w_{\ddot{r}}\Delta t^2/2 & 0 & 0 & 0 & 0 \\ w_{\ddot{r}}\Delta t^2/2 & w_{\ddot{r}}\Delta t & 0 & 0 & 0 & 0 \\ 0 & 0 & w_{r\ddot{\theta}}\Delta t^3/3 & w_{r\ddot{\theta}}\Delta t^2/2 & 0 & 0 \\ 0 & 0 & w_{r\ddot{\theta}}\Delta t^2/2 & w_{r\ddot{\theta}}\Delta t & 0 & 0 \\ 0 & 0 & 0 & 0 & w_{r\ddot{\phi}}\Delta t^3/3 & w_{r\ddot{\phi}}\Delta t^2/2 \\ 0 & 0 & 0 & 0 & w_{r\ddot{\phi}}\Delta t^2/2 & w_{r\ddot{\phi}}\Delta t \end{bmatrix}. \qquad (47)$$

Measurement Model— Since the purpose of this work is to begin the process of evaluating the feasibility of the decentralized control approach to distributed satellites, a very simple linear time-invariant measurement model corresponding to noise-corrupted measurements of geocentric radius, longitude, and latitude is assumed[1]. The assumed measurement model is

$$\mathbf{Y}_i^j = \mathbf{H}^j\mathbf{X}_i^j + \mathbf{v}_i^j, \qquad (48)$$

with $\mathrm{E}\left[\mathbf{v}_i^j\right] = \mathbf{0}$, $\mathrm{E}\left[\mathbf{v}_i^j(\mathbf{v}_\ell^j)^\mathsf{T}\right] = \mathbf{V}^j\delta_{i\ell}$, where

$$\mathbf{H}^j = \begin{bmatrix} 1 & 0 & 0 & 0 & 0 & 0 \\ 0 & 0 & 1/r_o & 0 & 0 & 0 \\ 0 & 0 & 0 & 0 & 1/r_o & 0 \end{bmatrix}, \qquad (49)$$

which is the same for all nodes. Recall that $\mathbf{X}^j(t)$ is the nonlinear state vector, whereas the controller operates on the state deviations, $\mathbf{x}^j(t)$. If the filter operates on the "measurement deviations," i.e.,

$$\mathbf{y}_i^j = \mathbf{H}^j\mathbf{X}_i^j + \mathbf{v}_i^j - \mathbf{H}^j\mathbf{X}_*(t_i) \qquad (50)$$

$$= \mathbf{H}^j\mathbf{x}_i^j + \mathbf{v}_i^j, \qquad (51)$$

then a linearized Kalman filter design results.

Modifications to LQ Design to Accommodate Decentralized Control Framework

For the decentralized control solution approach of reference [1], a single state space is assumed to be shared by all the nodes. Reference [3] shows that it is sufficient if each of the local state spaces may be linearly extracted from the global state space, e.g. $\mathbf{x}^j = \mathbf{T}\mathbf{x}$. In the context of the distributed satellite control problem, this condition is satisfied if the global state $\mathbf{x}$ is defined to be the column vector consisting of all the local states $\mathbf{x}^j$ arranged columnwise, e.g.

$$\mathbf{x}^\mathsf{T} = \left[(\mathbf{x}^1)^\mathsf{T}, (\mathbf{x}^2)^\mathsf{T}, \ldots, (\mathbf{x}^K)^\mathsf{T}\right]. \qquad (52)$$

The global state sensitivity matrix is then a block diagonal matrix with the (identical) local state sensitivity matrices along its diagonal.

The solution approach of reference [1] also requires that the local states be decomposed into $\mathbf{x}_i^{Cj}$, that depend only on the control, and $\hat{\mathbf{x}}_i^{Dj}$, that depend only on the incoming data. The Kalman filter design presented above operates on the entire state, as would all existing filter designs that might be used. To accommodate the need for $\hat{\mathbf{x}}_i^{Dj}$ in computing the control, $\mathbf{x}_i^{Cj}$ was computed external to the filter, and subtracted from the whole state output of the filter to get $\hat{\mathbf{x}}_i^{Dj}$.

4. Mission Simulation and Results

To begin to study the feasibility of the decentralized LQG control strategy described above to satellite formation flying, an example of a distributed satellite mission is considered. The example mission selected, which Figure 3 illustrates, could be of interest for making distributed sparse radar observations of earth-based targets, since the projection of the satellites' motion relative to one another onto a locally level plane is circular. Thus, the satellites appear to maintain constant baselines relative to an earth-based target. Perturbations to the two-body motion must be compensated in order to maintain desired configuration.

Since the purpose of this work is feasibility assessment only, the simulation model is identical to the design model used for the LQG controller, and all perturbations are Gaussian white noise processes. The commanded maneuvers are without execution error, and the measurements are bias-free. To complete the LQG design, the free parameters must be specified. After a few design iterations, the values indicated in Table 1 were selected, based on having generally adequate

[1]This is quite an unrealistic assumption, and in fact the primary manner in which time-varying systems enter the distributed satellite problem is through the measurements.

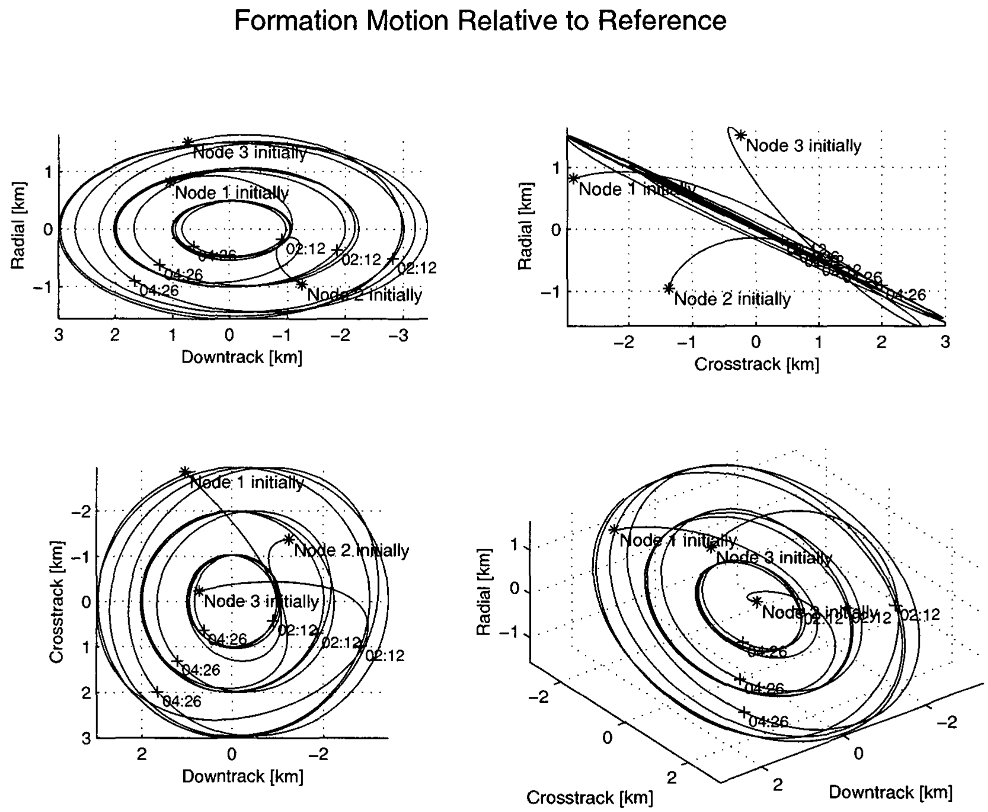

Figure 3: Controlled motion of distributed satellites. Upper left—in-plane motion cycles clockwise; upper right—out-of-plane motion constrained to inclined plane; lower left—motion viewed from zenith is circular; lower right—isometric view of motion

performance in terms of Eqs. (12)-(14). The reference orbit radius and the simulation time step are $r_* = 7178$ km and $\Delta t = 1$ min., respectively. Note that the measurements and maneuvers are assumed to be synchronized to occur on the simulation time steps.

Note that the use of a penalty function on the states along the path has been used (since $\mathbf{Q} \neq 0$), and a terminal penalty function has not used (since $\mathbf{S}_N = 0$). It has been more common when developing spacecraft maneuvers to use the opposite strategy, e.g. Lambert targeting and the Hohmann transfer, which provide only for meeting final constraints, and do not penalize deviations along the path from a desired trajectory. Such approaches might not be adequate for a tight satellite formation however, where collision and near-miss avoidance becomes an issue. In such a scenario, it could be essential that the vehicles remain close to their pre-planned trajectories, rather than take arbitrary Keplerian paths between current and desired final states.

During observation periods, it is likely that maneuvering may be inhibited for various reasons such as minimizing vibrational disturbances onboard the vehicles, preventing corruption of instruments from thruster plumes, etc. It is also possible that small, high specific-impulse thrusters would be used that would be pulsed at high rates, applying a small velocity increment to the vehicles at each pulse interval in order to accomplish maneuvers. Based on these assumptions, the simulation consists of three distinct time intervals: (1) an initial maneuver window lasting a little over one orbit (100 minutes) during which the satellites are initially driven onto the desired local reference trajectories, (2) an observation period lasting approximately two orbits during which no maneuvers are performed and perturbations tend to drive the satellites away from their desired local references, and (3) a final maneuver window lasting a little over one orbit (100 minutes) during which the satellites are driven back to their desired local references.

This strategy and its effects on the satellites is most clearly evident in Figure 4. The lowest subplot shows the commanded velocity increments, which are clearly zero during the observation period from about 01:40 to 05:00 hours. During this time, the position and velocity deviations that the upper sub-

Table 1: LQG Design Parameters

Parameter	Nomenclature	Value(s)
$\mathbf{Q}$	State Penalty Matrix	I
$\mathbf{R}^j$	Control Penalty Matrix	$\text{diag}(1.75e8, 1e8, 1e8)$
$\mathbf{S}_N$	Final State Penalty Matrix	$\mathbf{0}$
$\mathbf{V}^j$	Measurement Noise Covariance	$\text{diag}(50, 25, 25)$
$w_{\ddot{r}}, w_{r\ddot{\theta}}, w_{r\ddot{\phi}}$	Process Noise Spectral Densities	$9.81e-4$
$\mathbf{P}^j(t_o)$	Initial Covariance	$\sigma_r = \sigma_{r\theta} = \sigma_{r\phi} = 100$, $\sigma_{\dot{r}} = \sigma_{r\dot{\theta}} = \sigma_{r\dot{\phi}} = 0.1$, $\rho_{r,(r\dot{\theta})} = \rho_{(r\theta),\dot{r}} = -.9$, all other elements zero

plots depict gradually build up, but are driven back to zero during the final maneuver window. This plot is typical of the other nodes' performance, which must be ommitted here for brevity. For completeness, the performance of the navigation system is also illustrated by Figure 5. The filter's estimation errors remain within the filter's expected error region, and have the signature of uncorrelated errors. The filter's performance is not affected by the maneuvering that occurs during the first 01:40 hours and from 05:00 to 06:40 hours.

5. Conclusions

The decentralized control approach of reference [1] has been successfully applied to a simplified version of a distributed satellite contol problem. This constitutes a first step in the assessment of the feasibility of this method for use in satellite formation flying missions. Based on the promising results acheived with this phase of the feasibility assessment, further study of the implications of relaxing the simplifying assumptions used here are expected to be pursued.

Note that in the simplified formulation used in this paper, the local measurements are functions only of the local state. Also, the desired local trajectories are specified relative only to the formation center, and not with respect to the other nodes. Therefore, there is no advantage *from the control systems point of view* for information sharing. However, mission objectives such as coordination of observations or fleet reconfiguration could require each node to have knowledge of the states of all the other nodes. The decentralized framework provides an efficient means for communicating this information with minimal data transmission requirements. Also, in a realistic distributed spacecraft application, it is likely that relative measurements among the nodes would be utilized. In this scenario, the optimal local filter and therefore the optimal control requires knowledge of the states of all the nodes involved in the relative measurement.

Note also that the effects of command and data handling system and communications channel noise and latency must be considered. For example, it is likely that the measurement devices and/or their associated command and data handling systems may provide asynchronous and/or non-simultaneous measurement data. It is also probable that transmission of the data between nodes could be delayed one or more sampling periods and/or interrupted for extended intervals. Furthermore, since it is not possible to create a noise-free communications channel, errors in the transmitted data will be introduced at the level of the network, in addition to errors introduced at the measurement and state transition levels. An additional difficulty is that, in general, nonlinearities in the dynamics and measurements of the distributed satellite control problem require the use of ad-hoc procedures such as the extended Kalman filter.

References

[1] Speyer, J. L., "Computation and Transmission Requirements for a Decentralized Linear-Quadratic-Gaussian Control Problem," *IEEE Trans. Automat. Contr.*, vol. AC-24(2), pp. 266–269.

[2] Fan, C.-H., J. L. Speyer, and C. R. Jaensch, "Centralized and Decentralized Solutions of the Linear-Exponential-Gaussian Problem," *IEEE Trans. Automat. Contr.*, vol. AC-39(10), 1994.

[3] Willsky, A. S., et al., "Combining and Updating of Local Estimates and Regional Maps Along Sets of One-Dimensional Tracks," *IEEE Trans. Automat. Contr.*, vol. AC-27(4), pp. 799–813.

[4] Levy, B. C., et al., "A Scattering Framework for Decentralized Estimation Problems," *Automatica*, vol. 19(4), pp. 373–387.

[5] Kerr, T., "Decentralizeed Filtering and Redundancy Management for Multisensor Navigation," *IEEE Trans. Aerosp. Electr. Sys.*, vol. AES-23(1), pp. 83-119. Also, Kerr, T., "Corrections to 'Decentralizeed Filtering and Redundancy Management for Multisensor Navigation,'" *IEEE Trans. Aerosp. Electr. Sys.*, vol. AES-23(3), p. 412.

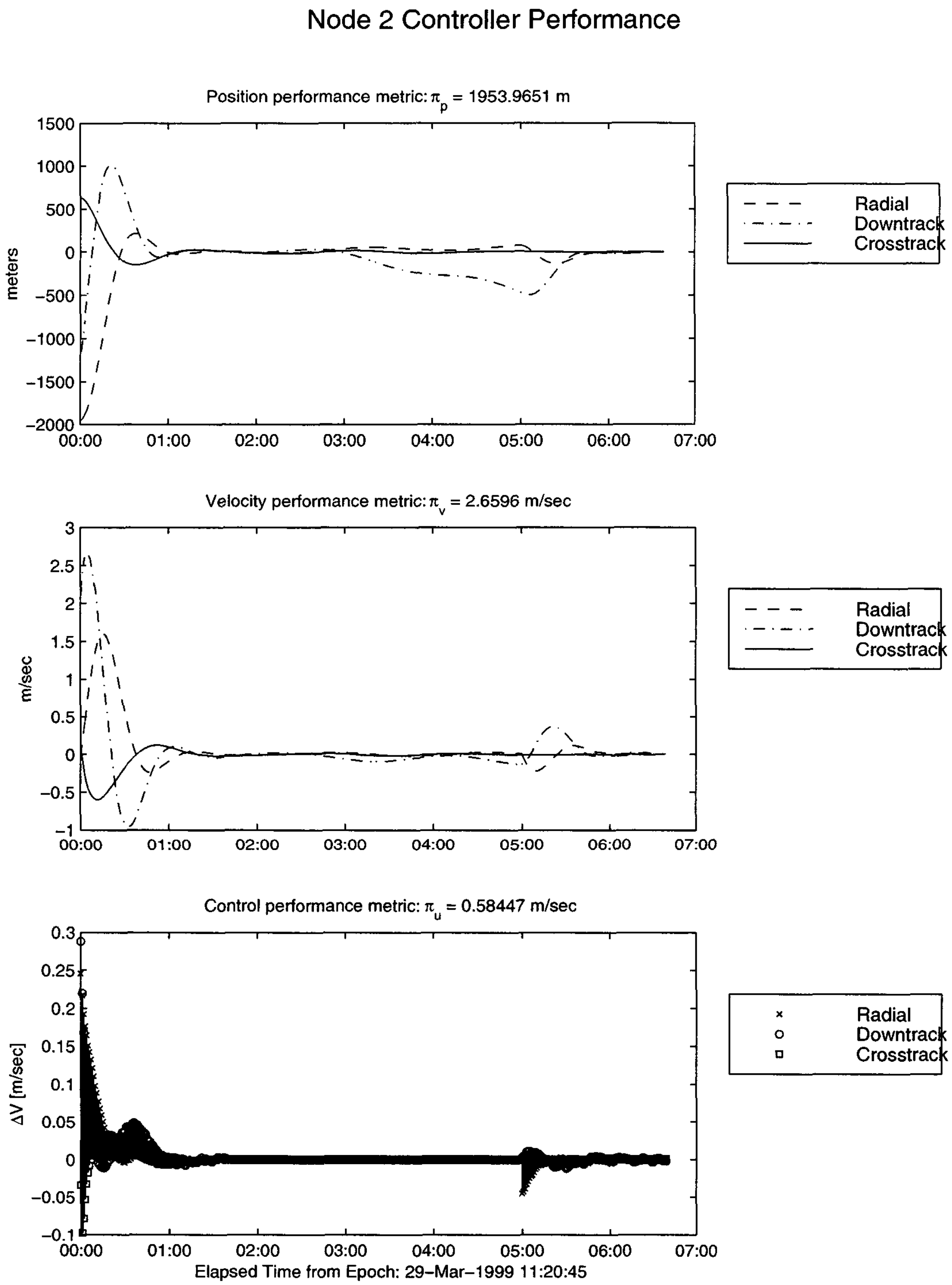

Figure 4: Controller performance (node 2), with maneuver windows during orbits 1 and 4. Upper and middle subplots—position and velocity deviations from desired local trajectory. Lowest subplot—velocity increments commanded by control law.

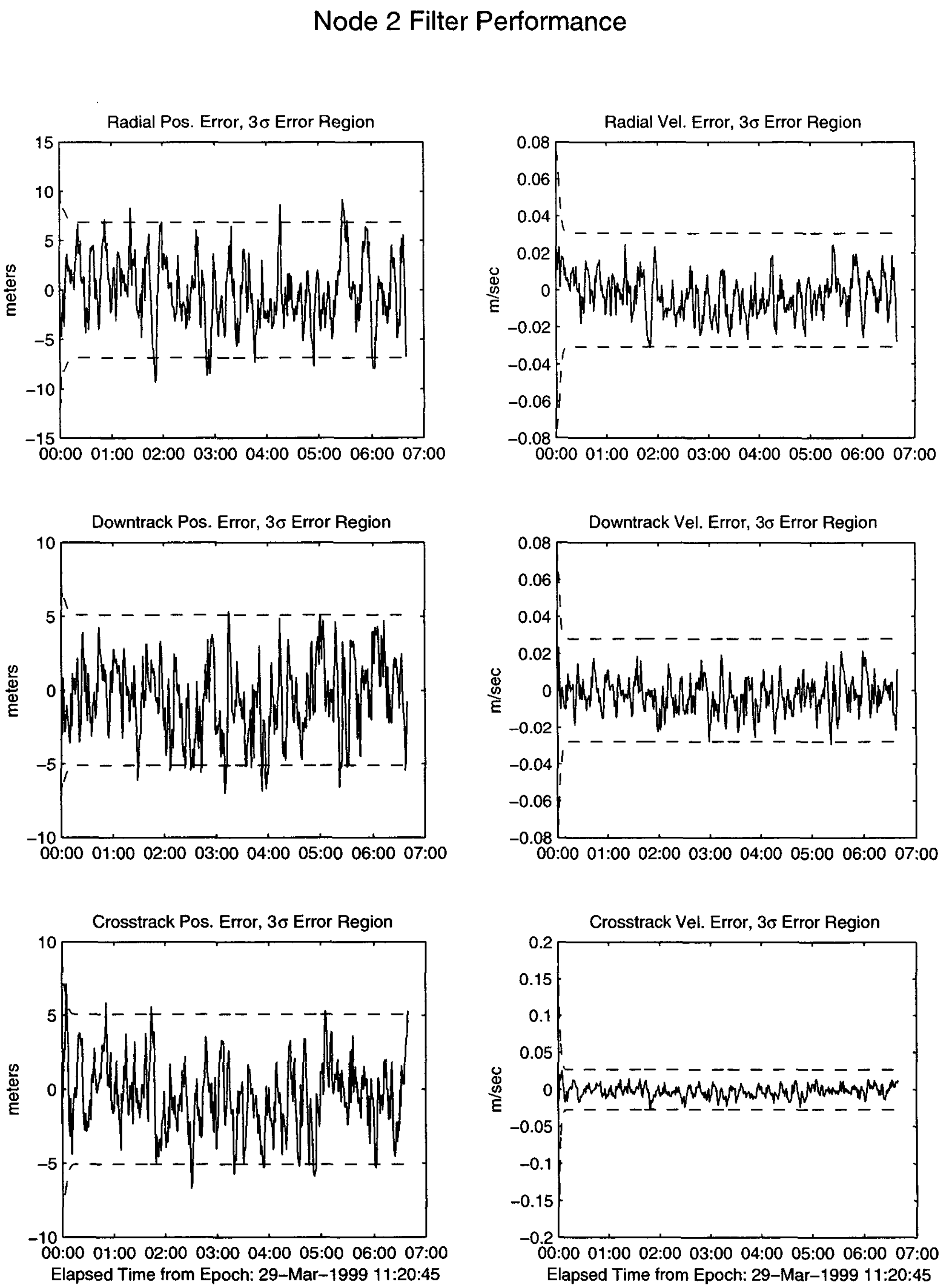

Figure 5: Filter performance for node 2

[6] Kaplan, M. H., *Modern Spacecraft Dynamics and Control*, Wiley, New York, 1976, pp. 109–115.

[7] Dorato, P., Abdallah, C., and Cerone, V., *Linear-Quadratic Control: An Introduction*, Prentice-Hall, Englewood Cliffs, NJ, 1995, pp. 44–50.

[8] Sabol, C., Burns, R., and McLaughlin, C. A., "Satellite Formation Flying Design and Evolution," Paper AAS 99-121, *AAS/AIAA Space Flight Mechanics Meeting*, Feb. 7–10, 1999, Breckenridge, CO.

[9] Kong, E. M. C., Miller, D. W., and Sedwick, R. J., "Exploiting Orbital Dynamics for Aperture Synthesis Using Distributed Satellite Systems: Applications to a Visible Earth Imager System," Paper AAS 99–122, *AAS/AIAA Space Flight Mechanics Meeting*, Feb. 7–10, 1999, Breckenridge, CO.

[10] Sedwick, R. J., Miller, D. W., and Kong, E. M. C., "Mitigation of Differential Perturbations in Clusters of Formation Flying Satellites," Paper AAS 99-124, *AAS/AIAA Space Flight Mechanics Meeting*, Feb. 7–10, 1999, Breckenridge, CO.

[11] Tan, Z., Bainum, P. M., and Strong, A., "A Strategy for Maintaining Distance Between Satellites in an Orbiting Constellation," Paper AAS 99-125, *AAS/AIAA Space Flight Mechanics Meeting*, Feb. 7–10, 1999, Breckenridge, CO.

Russell Carpenter *is an Aerospace Engineer at NASA Goddard Space Flight Center, where he has worked in the Guidance, Navigation, and Control Center since July of 1998. His current research areas involve formation flying GN&C and GPS development, analysis, simulation, and test. Before coming to NASA Goddard, Dr. Carpenter was at NASA Johnson Space Center from 1987–1998, where his research involved development, analysis, simulation, and test of space flight navigation techniques, future exploration missions, and advanced technology experiments. Dr. Carpenter attended The University of Texas at Austin, receiving his B.S., M.S., and Ph.D. in Aerospace Engineering in 1989, 1991, and 1996, respectively.*